INCORPORATING SECONDARY PHASES IN 3D REGIONAL SEISMIC EVENT LOCATION: APPLICATION TO THE SPARSE NETWORK PROBLEM

Delaine Reiter, Jessie L. Bonner, Carolynn Vincent, and James Britton

Weston Geophysical Corporation

Sponsored by Defense Threat Reduction Agency

Contract No. DTRA01-00-C-0098

ABSTRACT

One of the most important issues in nuclear explosion monitoring is the accurate location of small seismic events that may only be recorded on a sparse, regional network. To address this problem, we have developed a method of regional seismic event location that fully incorporates 3D velocity models and travel-time prediction for multiple phase arrivals. To estimate event hypocenters, we utilize the 3D grid search location algorithm of Rodi and Toksöz (2001). This location method generates 3D Monte Carlo confidence regions in addition to the hypocentral parameters. We calculate station-centered travel- time grids for use in the location estimates via the 3D Podvin-Lecomte (1991) finite-difference method. We have extended the Podvin-Lecomte method to generate travel times for secondary regional phases such as *Pg, Sn* and depth phases (*pPn, sPn*, etc.). The resulting algorithm is unique in its ability to locate events using fully 3D models and all regional primary and secondary body-wave phase arrivals.

To demonstrate the technique, we have applied it to events recorded in Pakistan and the surrounding region. We identified events in the EHB bulletin (Engdahl *et al.*, 1998) that were well-recorded teleseismically ($mb \geq 4.1$) and had recorded multiple teleseismic depth phase picks and at least one regional depth phase pick. We relocated these events using the phase arrival data from four International Monitoring System (IMS or IMS surrogate) stations in the Pakistan region and our tomographically derived, 3D *P*-wave velocity model (WINPAK3D) for the area (Reiter *et al*., 2001). Using various combinations of regional *P, S,* and *pP* phase picks from this sparse network configuration, we have calculated hypocentral estimates and their associated Monte Carlo confidence regions. The results of these tests clearly indicate that even one regional depth phase pick can significantly improve depth accuracy and decrease the size of the hypocentral confidence regions. This improvement is particularly pronounced for events occurring at crustal and upper mantle depths that are of interest to nuclear monitoring agencies. The addition of shear phases can also improve the location estimates but is dependent on the accuracy of the *S* wave picks, which typically have more error than *P* wave picks.

OBJECTIVE

The overall objective of this research program is to produce a fully 3D grid-search location algorithm that can more accurately locate seismic events using the International Monitoring System (IMS) network. Within this framework we are investigating a number of extensions and applications of our basic algorithm, which is a regional event location method that incorporates 3D velocity models and travel-time predictions into a nested grid-search location technique. In this paper we investigate the improvements in the hypocentral and confidence region estimates that occur when we utilize both primary and secondary phases, and apply the resulting algorithm to the uncertainties associated with sparse regional network locations. Specifically, we apply our 3D model-based, grid-search location algorithm to five- and four-station network locations for events from southern Asia to examine how well we can determine event depths using various combinations of regional arrivals. The goal of our study is to show that the addition of secondary phases, in particular depth phases, can significantly increase the accuracy and confidence of sparse network depth estimates.

RESEARCH ACCOMPLISHED

Regional Event Location in 3D Models using Secondary Phases

One of the most important nuclear test-monitoring problems facing seismologists is the accurate location and identification of small seismic events that may not be recorded at teleseismic distances. In cases where the events are only recorded at regional distances on what will likely be a sparse network, with five or fewer stations and a large azimuthal gap, the accuracy of the velocity model and the incorporation of secondary phase arrivals are critically important to obtaining a valid location.

We have been developing a network location algorithm that incorporates 3D regional travel-time prediction with a Grid-search Multiple Event Location algorithm (GMEL) developed at M.I.T. (Rodi and Toksöz, 2000, 2001). The algorithm employs a recursive grid-search technique to find the best-fitting location parameters (origin time and hypocenter) of an event, and a Monte Carlo technique to obtain confidence regions on the location parameters. These numerical techniques avoid many of the restrictive assumptions and approximations used in conventional location algorithms (e.g., Geiger's method (Geiger, 1912)), but they are more computationally intensive.

To generate the synthetic travel times for GMEL, we use the Podvin and Lecomte (1991) method, which solves the travel time problem in a 3D medium using a finite difference approximation of Huygens' principle. The Podvin-Lecomte (P-L) method is capable of accurately modeling different propagation modes, such as transmitted and diffracted body waves or head waves. This method can provide accurate travel times in the presence of extremely severe, arbitrarily shaped velocity contrasts. Podvin-Lecomte travel-time prediction is an improvement over other similar methods (Vidale, 1990; Moser, 1991), which can encounter serious difficulties in the presence of sharp first-order contrasts. The velocity model is set up as a uniform grid in three dimensions, and first arrival travel times from each station are computed to each point within the grid. This method of travel time computation is considerably faster than two-point ray tracing in a 3D model, and the sources and receivers can be located anywhere within the model.

The grid-search location method (GMEL) has been modified to utilize any phase arrivals for which there are travel-time tables. To exploit this functionality with 3D velocity models, we have extended the method of P-L to allow us to predict travel times for regional secondary phases such as *Pg, pPn, sPn* and *Sn.* For the most prominent regional shear wave phase, *Sn*, there are no modifications necessary in the P-L code. All that is required is to input the appropriate shear wave velocity model and run the P-L code in its original mode.

Secondary regional phases such as *Pg* and *Sg* (or *Pb* and *Sb*) require a modification of the input velocity models prior to running the P-L code. For *Pg* and *Sg* phases, we ensure that the travel times are either that of an upgoing wave from a source in the upper crust or a wave bottoming in the upper crust. Therefore, for *Pg* or *Sg* phases we 'mask' the 3D velocity model below the uppermost crustal layer, provided there is such a demarcation in a given model. For *Pb* or *Sb* phases, the model 'masking' begins below the Moho to ensure that the waves are either originating in the lower crust or bottoming in the lower crust. Our modification entails replacing the velocity models below the appropriate layer with a very slow constant velocity and running the P-L code in its original format. For demonstration purposes, we show travel time calculation results in Figure 1 for the 1-D IASPEI model

(Kennett and Engdahl, 1991) that has both upper and lower crustal layers. The reduced travel times generated by P-L for *Pg*, *Pb*, and *Pn* are shown as a function of epicentral distance for a surface focus event (squares for *Pn*, triangles for *Pb* and diamonds for *Pg*). These travel times are compared to the analytical times (the lines underlying the respective markers) expected from the IASP91 model (Buland and Chapman, 1983). The fit is excellent for all phases, demonstrating that the P-L method can accurately produce secondary phase arrivals for use in a location routine. However, in the EHB (Engdahl *et al*., 1998) event bulletin, there are very few travel time picks for *Pg, Pb, Sg* or *Sb* designated as secondary phases, and none of these picks were utilized in producing event locations in the EHB database. Therefore, we currently do not produce independent secondary phase *Pg, Pb, Sg* or *Sb* tables for use in our location routine.

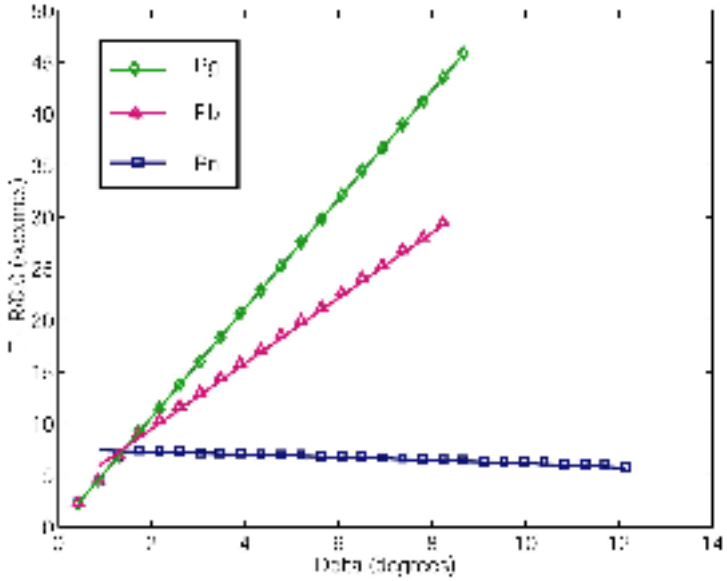

Figure 1. Reduced travel times from the IASP91 model as a function of epicentral distance for a surface focus event. The analytical times are plotted as lines, and the overlying markers are the travel times predicted by the P-L finite difference method for phases *Pn*, *Pb*, and *Pg*. The numerical technique accurately predicts the arrival times of the secondary phases.

The most extensive modification of the 3D travel-time prediction software is required to predict the arrival times for the depth phases such as *pPn* and *sPn*. For these phases, a two-part calculation is necessary to predict travel times from a particular station to points throughout the model. The first part of the calculation generates travel times from the station to every point in the travel time grid (corresponding to the "*P*" leg of a "*pP*" depth phase, for example). In the second part of the calculation, the travel time grid is reinitialized to contain only travel times from the surface of the first grid, and the P-L code is run again to generate the total depth phase travel times and complete the surface-to-event bounce portion of the path (the "*p*" leg of the "*pP*" depth phase) to all remaining points in the grid. Figure 2 shows a simplified schematic of the two-part process that generates depth phase arrival times using the 3D Podvin-Lecomte finite difference algorithm.

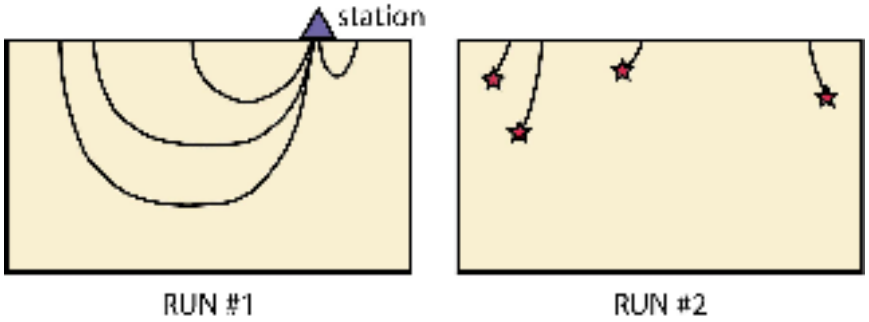

Figure 2. Simplified 2D schematic of method used to generate depth phase arrival times using the 3D Podvin-Lecomte finite difference method. The first run (on the left) generates times from the station to every point on the surface of the travel time grid. The second leg is initialized with the times from the first run, and the code is then used to generate the complete depth phase arrival times to all possible event points in the grid.

With the modifications to the P-L and GMEL codes to predict the travel times of depth phases and shear phases completed, we have the ability to include the secondary phase picks in regional location estimates. In the next section we first examine the accuracy of using only primary arrivals to estimate depth accuracy from sparse regional networks for a subset of events with well-constrained focal depths. Then we investigate how we can improve the depths by including the secondary phase arrivals in the location estimation.

Application to Depth Estimation Using a Sparse Network in Southern Asia

Successful monitoring of nuclear testing activity requires the accurate characterization of all recorded signals and the identification of any suspicious events that may be clandestine nuclear explosions. A definitive way to rule out a majority of seismic events as possible nuclear tests is to accurately determine that the source depth is greater than 15 km, as the practical limit of drilling and explosion emplacement is on the order of a few kilometers. However, depth determination still remains one of the most challenging problems for seismic monitoring, because variations in the depth of a seismic event can cause travel time differences that are indistinguishable from changes in the event's origin time. The problem is made more difficult for small events ($m_b < 4$) that are only recorded at regional distances on sparse networks. A regional location method that can more accurately determine depths for these small events would be a valuable resource for nuclear monitoring agencies. For that reason, we have applied our new 3D regional location technique that can incorporate secondary phases to the sparse network problem in Southern Asia.

Our first goal was to determine the depth location capabilities of a pseudo-IMS network in Southern Asia using only *P*-wave arrivals from four- and five-station networks. To complete this objective, we first compiled a test dataset of seismic events with accurate focal depths determined from multiple teleseismic depth phases. We examined the Center for Monitoring Research's (CMR) Reference Event Database (REDB) for events between 1995 and 2000 that occurred within the bounds of WINPAK3D, the Weston INdia and PAKistan regional 3D velocity model (Reiter *et al.,* 2001) that is bounded by 12° and 43° north latitudes and 55° and 80° east longitudes. Of the resulting 108 events, only 38 events had five or more teleseismic depth phases and were not used in the tomographic update of the WINPAK3D model (Reiter *et al*., 2001). We then cross-referenced the remaining candidate events with the EHB bulletin (Engdahl *et al*., 1998) and searched for events with at least five regional *P* arrivals. The resulting test dataset (Figure 3 and Table 1) includes 23 events with accurate focal depths that were used for our sparse network locations.

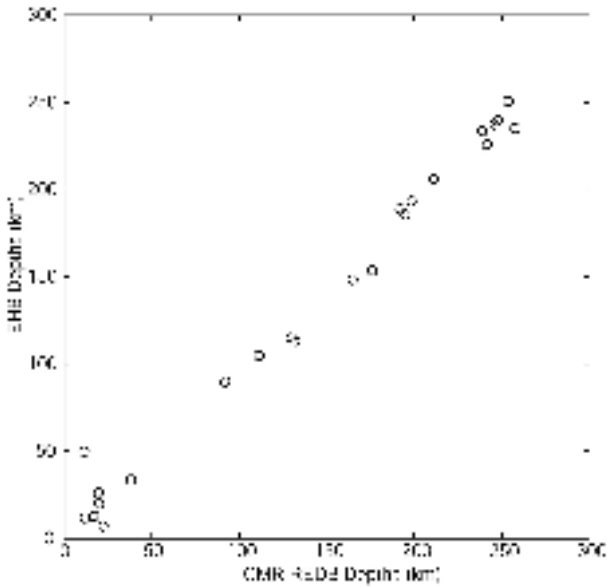

Figure 3. Depth comparison for the CMR REDB and EHB published depths for the 23 test events. The CMR REDB depth is based on five or more teleseismic depth phases and was chosen for the reference depth in this study.

Table 1. CMR REDB and EHB origin parameters for the test dataset.

CMR REDB								EHB			
Date	OT	Lat	Long	Z	mb	Depth Phases	EVID	OT	Lat	Long	Z
1/29/1995	1:20:13	36.84N	71.51E	111.1	4.9	7	303866	1:20:13	36.9367	71.532	104.8
5/16/1995	3:35:04	36.44N	70.95E	192	5.3	28	321673	3:35:04	36.4507	70.909	188.8
6/25/1995	6:38:33	37.91N	72.92E	164.8	4.7	5	328713	6:38:32	37.9485	72.984	148.4
8/17/1995	23:14:21	36.35N	71.14E	245.8	5.3	13	337013	23:14:21	36.4357	71.122	237.3
10/8/1995	8:55:48	40.93N	72.03E	22.2	5.7	29	345874	8:55:46	41.0025	72.155	7
10/18/1995	9:30:41	36.35N	70.39E	241.4	5.7	69	348234	9:30:40	36.4317	70.389	225.8
7/24/1996	17:23:54	35.91N	68.50E	11.5	5	21	402331	17:24:00	35.9838	68.61	49.8
9/14/1996	8:01:06	35.93N	70.66E	132.1	5.4	15	411509	8:01:05	36.0088	70.701	113.1
11/30/1996	11:02:50	36.30N	71.00E	253.6	4.6	30	424565	11:02:50	36.3636	71.036	250.6
3/19/1997	11:15:49	30.23N	67.93E	17.1	4.2	19	441655	11:15:50	30.3104	67.991	12.7
4/21/1997	9:16:24	36.93N	71.78E	176	4.8	5	447150	9:16:23	37.0359	71.835	153.4
5/15/1997	18:30:27	36.40N	70.85E	194.9	5.1	14	451554	18:30:26	36.4537	70.884	185.7
5/17/1997	3:07:30	29.65N	68.20E	11.8	4.4	8	451765	3:07:31	29.7014	68.179	11.8
5/17/1997	3:58:24	39.57N	76.92E	19.5	4.6	17	451769	3:58:25	39.5178	76.936	26
8/6/1997	15:00:12	36.43N	70.85E	198.4	4.7	22	464332	15:00:12	36.4668	70.873	193.4
8/9/1997	17:05:29	36.54N	60.38E	38.1	4.1	6	464801	17:05:28	36.5509	60.362	33.7
9/7/1997	10:15:25	29.96N	67.76E	20	5	27	469157	10:15:25	29.9813	67.771	20
11/1/1997	3:46:36	36.38N	70.74E	211.1	5.1	15	478539	3:46:35	36.4257	70.695	206.1
2/20/1998	12:18:10	36.54N	71.07E	257.6	5.8	22	249066	12:18:08	36.4537	71.074	235
3/6/1998	10:51:11	38.30N	73.35E	129.6	4.1	8	251346	10:51:09	38.293	73.383	114.8
3/9/1998	23:21:37	36.60N	71.08E	238.8	4.3	21	251914	23:21:36	36.4758	71.082	233.5
3/21/1998	18:22:32	36.37N	70.18E	247.7	5.9	16	253834	18:22:31	36.4157	70.136	239.5
6/10/1998	8:30:16	28.14N	58.46E	92	4.7	21	269821	8:30:15	28.1578	58.48	89.8

The first goal of this study was to empirically determine the depth estimation capabilities of a sparse network in southern Asia using only the first-arriving *P*-wave travel times. Thus, we relocated the events in Table 1 using only P-wave arrivals from four- and five-IMS stations in the region (Figure 4) including NIL (or nearby station CHCP), ABKT (previously ASH), and AAK (previously FRU). Two other IMS stations in the region are COC and KRM; however, data from these stations are not yet available, and thus surrogates were used for the relocations. For the station COC, the Indian stations HYB, POO, or NDI were used as directional surrogates, and QUE was used for the Iranian station KRM. Note that the results presented in this paper do not represent the final capabilities of the IMS network in this region; however, they do provide initial insight into the depth estimation capabilities of this sparse network. We relocated our database of 23 events using the GMEL algorithm with WINPAK3D as the velocity model.

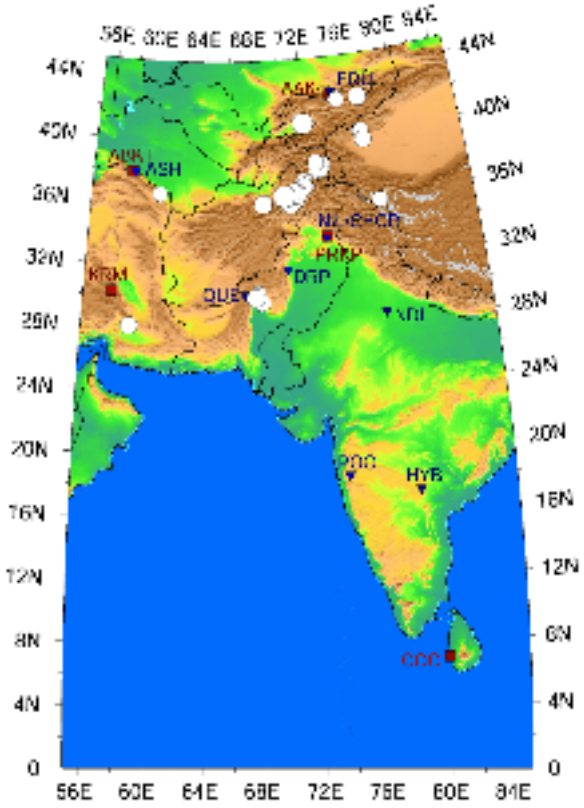

Figure 4. Locations of the test events (white circles), IMS stations (red squares) and surrogates (blue triangles) used in the four- and five-station 3D regional location study.

The results of the five IMS station locations are shown on the left side of Figure 5. The depth mislocation, determined as the difference between the maximum likelihood depth found by GMEL and the CMR REDB depth (Table 1), was less than 35 km for 21 out of the 23 events. Four of the 23 events (22%) had depth mislocation less than 10 km, while eight events had mislocation between 10 and 20 km. The mean depth mislocation was 27 km, and is only 18 km if the two outlier events are eliminated from the calculation. We also note that all CMR REDB depths fell within the 95% confidence interval determined from Monte Carlo simulations inherent in the grid-search algorithm. These results suggest that depths for events recorded on at least five regional stations in southern Asia will be very reliable.

The results for the four IMS station locations (Figure 5, right side) are not as promising. Only one of the 23 events had a depth mislocation less than 10 km and more than 75% of the events (18) had mislocation greater than 35 km. The mean depth mislocation increased to 88 km, and several of the CMR GTDB depths fell outside of the 95% confidence intervals determined from the grid-search algorithm. These results suggest that depths calculated for small events recorded only on four IMS stations in southern Asia will not be reliable. This implies that secondary

phases, and in particular depth phases, will be necessary to resolve the depths for many small events in southern Asia recorded by 4 or fewer stations.

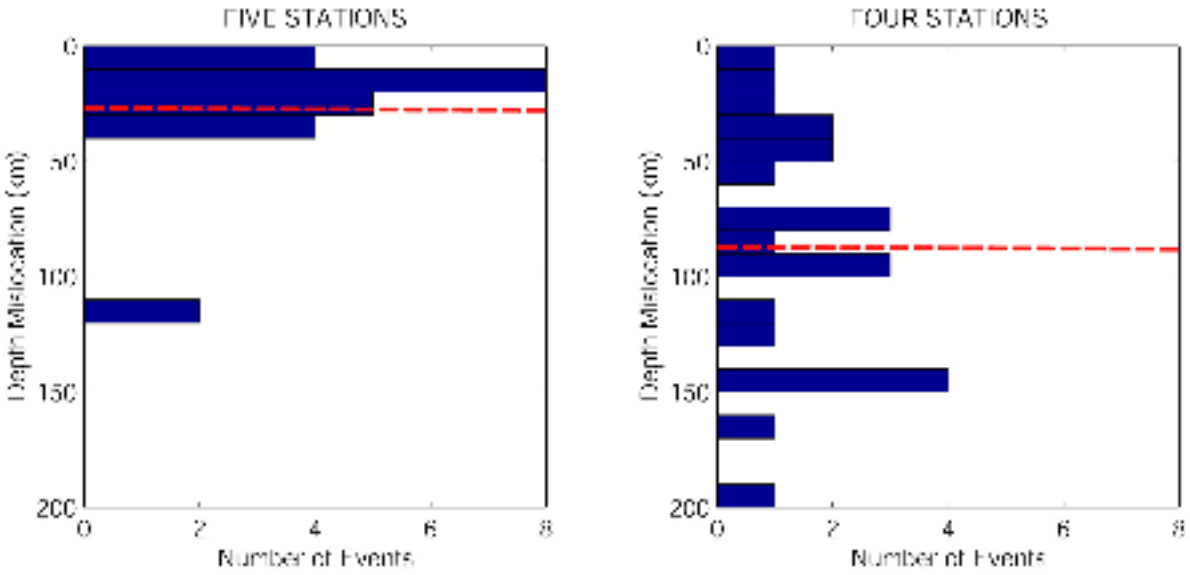

Figure 5. Histograms showing the depth mislocation for five (left) and four (right) station locations. The mean mislocation error is shown as the dashed red line.

To illustrate the effect of adding reliable depth phase picks on the hypocenter and confidence region estimates, we relocated the 23 events in Table 1 using the modified version of GMEL and any available secondary phases. However, of the 23 events in our database, none had regional depth phase picks (distances less than 15°) in the EHB database, although 15 of the 23 events have *pP* picks, nearly all of them at station HYB at epicentral distances between 16 – 22°. We note that this absence of regional depth phases (less than 15°) is by design for the EHB database. We then used cepstral techniques (Bonner *et al*., 2002a) in an attempt to detect and pick regional depth phases from the events listed in Table 1 as recorded at ABKT/ASH, AAK/FRU, NIL, and HYB. For example, Figure 6 shows the 4-station network geometry for an event from Table 1 (EHB database EVID 469157). This event was located at 20 km depth by both the CMR REDB and EHB bulletins, and neither bulletin had regional distance depth phase picks. Using the cepstral technique, we were able to pick *pPn* at stations ABKT/ASH and AAK/FRU (Bonner *et al*., 2002b). *Sn* picks were also available at stations AAK, NIL and NDI, giving a total of nine primary and secondary phase arrival times to utilize in relocating the event.

The hypocenters and Monte Carlo confidence regions found by GMEL using two subsets of the 4-station regional dataset for EVID 469157 are shown in Figure 7. The results from locating with the four *Pn* arrivals from each station are shown in the top row, and the bottom row shows the results found by including the two *pPn* arrivals at FRU and ASH with the four *Pn* arrivals at all stations. The left-hand columns are projections of the epicentral confidence region, while the right two columns are depth slices of the confidence regions through the best-fitting hypocenter. The CMR REDB "ground-truth" location is shown on each subplot as a white-filled circle that has an estimated accuracy of ± 15 km (shown as dashed green circles surrounding the CMR REDB location), and the minimum rms hypocenter from GMEL is shown as a white cross. We do not show the other two subsets of results (locations done with the *Pn* and *Sn* or with all of the *Pn*, *pPn* and *Sn* arrivals), because adding the *Sn* arrivals does not substantially affect the results in this case.

The results indicate that adding the two depth phase arrivals significantly improves the depth estimates for this event. The minimum-rms depth estimate from GMEL using only the four *Pn* arrivals is 163 km, giving a depth mislocation error of 143 km from the CMR REDB and EHB estimates, and the confidence regions indicate that the event depth could range anywhere from the surface to greater than 200 km. However, the addition of two depth phase picks at FRU and ASH produces a GMEL depth estimate of 13 km (i.e. a depth mislocation error of 7 km), and the confidence intervals tightly constrain the depth of the event to be between approximately 0-30 km.

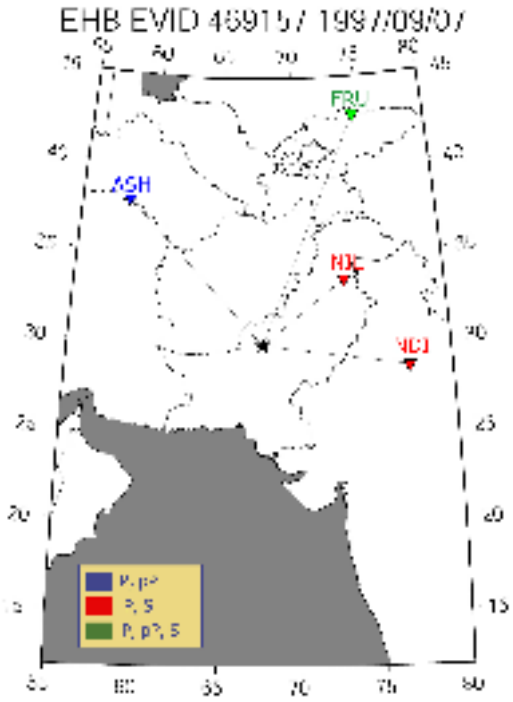

Figure 6. Four station regional network used to relocate Event No. 469157 from Table 1. The legend indicates which phase picks were available at a given station. Regional distance depth phases at stations ASH and FRU were picked using the cepstral F- statistic method of Bonner *et al.* (2002a).

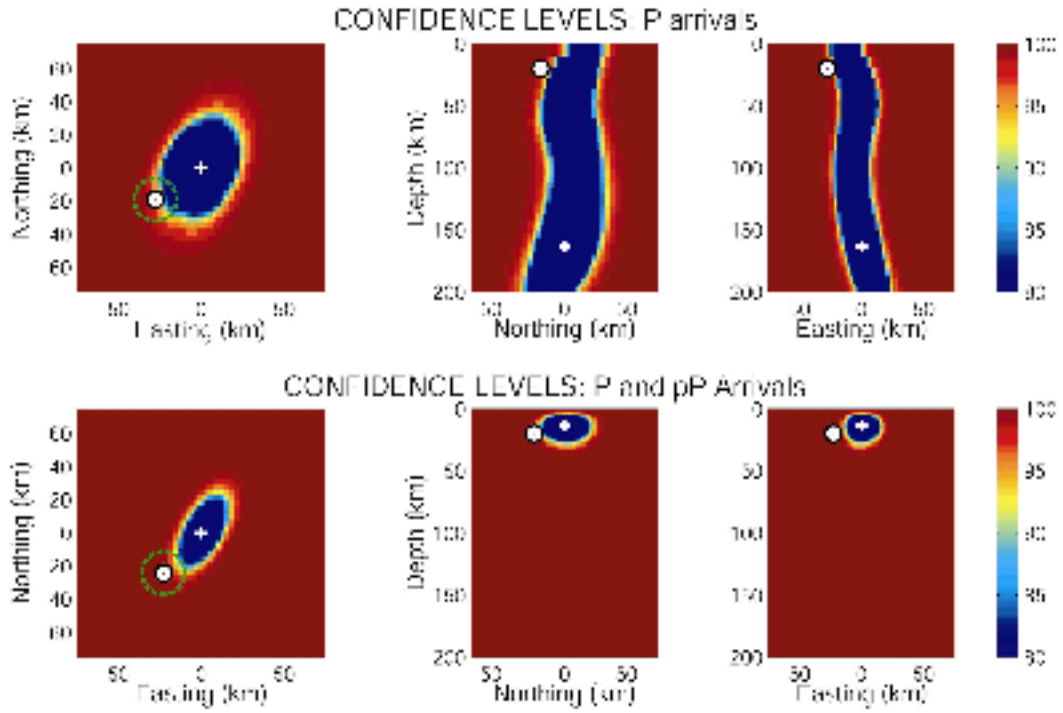

Figure 7. Hypocenter and confidence level estimates for two different sets of arrival picks from Event 469157. Top row: the event location using four *Pn* phase picks. Bottom row: the event location using four *Pn* picks and two *pPn* picks. The left-hand columns show the projections of the epicentral confidence regions, and the middle and right columns show depth slices through the minimum-rms hypocentral confidence regions. The white circles represent the CMR REDB "ground-truth" location (with the dashed green outer circles indicating the ±15 km accuracy of the published epicenter), and the white crosses are the minimum-rms locations found using GMEL.

CONCLUSIONS AND RECOMMENDATIONS

We have developed a fully 3D regional location algorithm that can utilize secondary phases such as *Pg, Sn* and depth phases (such as *pP, sP*) to better constrain network-derived hypocenter estimates. This location method is unique in that it utilizes grid search techniques, 3D velocity models and fully 3D travel-time prediction for primary and secondary phases to find the event hypocenters, and the method also produces Monte Carlo confidence regions on the location parameters. While the method of using 3D travel-time tables for secondary phases is currently developed using the location program GMEL, it can easily be integrated with routine location algorithms at the IDC by converting travel-time prediction tables to Source Specific Station Corrections (SSSCs) for each regional phase (*Sn, pPn, pSn*, etc). In this paper we applied the new location method to the problem of accurately determining the depth of events recorded regionally on a sparse network. To accomplish this objective, we investigated the depth estimation capability of four- and five-station regional network configurations using a subset of events from southern Asia with pre-existing, accurate focal depths.

Our location results suggest that regional depth phases will be necessary to resolve the depths for many small events in southern Asia and elsewhere when four or fewer stations record the event. Identification of depth phases, such as *pP* and *sP*, is dependent upon the amplitude of the arrival at a recording station. Source mechanism, path effects and reflection coefficients at the earth's surface control the depth phase amplitude as well as the amplitude of the *P* wave coda within which the depth phase will appear. When depth phases from an event are detected, an accurate source depth can be found by using the delay times of the depth phases relative to the *P* wave and the velocity profile near the source. Regional depth phase detection is extremely difficult because of the complexity of the regional seismogram and *P*-wave coda. Figure 8 verifies this fact by showing the depth phase detections listed in the Prototype International Data Center's (PIDC) Reviewed Event Bulletin (REB) for 1999. Less than 1% (45) of the 8072 *pP* picks were for stations at regional (less than 20°) distances.

Some of the currently available techniques to determine source depth from available depth phase data include body wave modeling (Goldstein and Dodge, 1998; Saikia and Helmberger, 1997), beamforming (Woodgold, 1999; Murphy *et al*., 1999), and relative amplitude techniques (Pearce, 1977). The cepstrum is another method that has been used in the past (Alexander, 1996 and Kemerait and Sutton, 1982) to detect depth phases in seismic data. We have used a cepstral F-statistic technique (Bonner *et al*., 2002b) in an attempt to detect regional depth phases from the events listed in Table 1 as recorded at ABKT/ASH, AAK/FRU, NIL, and HYB. Our results indicated that the

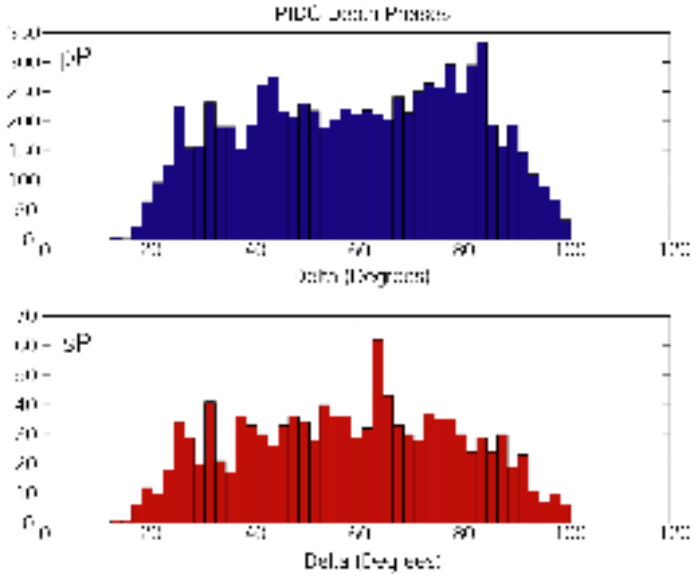

Figure 8. Depth phase (*pP*-top and *sP*-bottom) detections as a function of epicentral distance for the 1999 PIDC REB.

method was very successful at detecting regional depth phases at the stations HYB and ABKT/ASH. The method was less successful at AAK/FRU and NIL, because both stations were often located at near-regional distances to the events where the depth phases were masked by large secondary arrivals, or because the events were too deep to record regional depth phases. The results from this limited study suggest that regional depth phase arrivals are present in the data and a more concentrated effort is needed by analysts to pick these important phases. If the regional depth phases can be found with reliable accuracy, our location results indicate that they can be extremely helpful in improving the depth estimates from sparse network locations of regional events.

ACKNOWLEDGEMENTS

We are indebted to Bill Rodi for his GMEL program and helpful advice on this project. Bob Engdahl provided the latest version of the EHB bulletin, which we have used extensively in this study and others. We thank Xiaoping Yang for help in acquiring the statistics on depth phase detections at the pIDC. We also thank Anca Rosca for programming support and Shelly Johnson for help with the manuscript.

REFERENCES

Alexander, S. S. (1996), A new method for determining source depth from a single regional station, *Seismic Res. Letts*, 67, 63.

Bonner, J.L., D. T. Reiter, and R. H. Shumway (2002a), Application of a cepstral F statistic for improved depth determination, accepted to the *Bull. Seism. Soc. Am.*

Bonner, J. L., D. R. Reiter, and C. Vincent (2002b), Depth determination using sparse networks in southern Asia, in the *Conference Proceedings of 4th Annual Conference on Location Calibration and Event Screening*, 22-26 April 2002, Oslo, Norway.

Buland and Chapman (1983), The Computation of Seismic Travel Times, *Bull. Seism. Soc. Am*, 73, 1271-1302.

Engdahl, E. R., R. van der Hilst, and R. Buland (1998), Global teleseismic earthquake relocation with improved travel times and procedures for depth determination, *Bull. Seism. Soc. Am.,* 88, 722-743.

Geiger, L. (1912), Probability method for the determination of earthquake epicenters from the arrival time only, (translated from Geiger's 1910 German article), *Bulletin of St. Louis University*, 8 (1), 56-71.

Goldstein, P. and D. Dodge (1998), Depth and mechanism estimation using waveform modeling, in *Proceedings of the 20th Annual Seismic Research Symposium on Monitoring a Comprehensive Test Ban Treaty (CTBT)*, 238-247 (September 1998).

Kemerait, R. C. and A. F. Sutton (1982), A multidimensional approach to seismic event depth estimation, in *Geoexploration*, 20, 113-130.

Kennett, B.L.N. and E.R. Engdahl (1991), Traveltimes for global earthquake location and phase identification, *Geophys. J. Int.* 105, 429-465.

Moser, T.J. (1991), Shortest path calculation of seismic rays, *Geophysics*, 56, 59-67.

Murphy, J. R., R. W. Cook, and W.L. Rodi (1999), Improved focal depth determination for use in CTBT monitoring, *Proceedings of the 21st Annual Seismic Research Symposium: Technologies for Monitoring the Comprehensive Nuclear-Test-Ban Treaty (1999).*

Pearce, R.G. (1977), Fault plane solutions using relative amplitudes of *P* and *pP*, *Geophys. J. R. astr. Soc*., 50, 381-394.

Podvin, P. and I. Lecomte (1991), Finite difference computation of travel times in very contrasted velocity models: a massively parallel approach and its associated tools, *Geophys. J. Int*., 105, 271-284.

Reiter, D., W. Rodi, M. Johnson, C. Vincent, and A. Rosca (2001), A new regional velocity model of the India-Pakistan region,*Proceedings of the 23rd Seismic Research Review: Worldwide Monitoring of Nuclear Explosions*-October 2-5 2001, 305-314.

Rodi, W. and M. N. Toksöz (2000), Grid-search techniques for seismic event locations, *Proceedings, 22nd Annual DoD/DOE Seismic Research Symposium*, New Orleans, Louisiana (September 2000).

Rodi, W., and M.N. Toksöz (2001), Uncertainty analysis in seismic event location, *Proceedings, 23rd Seismic Research Review: Worldwide Monitoring of Nuclear Explosions*, Jackson Hole, Wyoming (October 2001).

Saikia, C.K. and D. V. Helmberger (1997), Approximation of rupture directivity in regional phases using upgoing and downgoing wave fields, *Bull. Seism. Soc. Am.,* 87, 987-998.

Vidale, J. (1990), Finite-difference calculation of traveltimes in three dimensions, *Geophys.,* 55, 521-526.

Woodgold, C. R. D. (1999), Wide-aperture beamforming of depth phases by timescale contraction, *Bull. Seis. Soc. Am*., 89, 165-177.